Int. J. Heat Mass Transfer. Vol. 28, No. 11, pp. 2061–2070, 1985
Printed in Great Britain

0017–9310/85 $3.00 + 0.00
Pergamon Press Ltd.

Mass transfer of trace species from a superheated stream to a subcooled surface

R. K. AHLUWALIA and K. H. IM
Engineering Division, Argonne National Laboratory, 9700 S. Cass Avenue, Argonne, IL 60439, U.S.A.

(*Received* 27 *November* 1984 *and in final form* 6 *May* 1985)

Abstract—The influence of boundary-layer nucleation on mass transfer of a condensable species from a superheated stream to a subcooled surface is analyzed. The concentration of the species is sufficiently dilute to preclude any condensation on the nucleated particles. It is found that a high supersaturation ratio is required to initiate the boundary-layer nucleation. As a consequence, the critical surface temperature for onset of nucleation and appearance of fog is much below that determined from a thermodynamic criterion. The vapor mass transfer is always depressed by boundary-layer nucleation. The subsequent deposition of nucleated particles in laminar flow more than compensates for the decrease so that the net mass transfer—vapour plus particle—exceeds the value obtained from disregarding the nucleation. For turbulent flow, the net mass transfer decreases because of boundary-layer nucleation in part due to the turbulent diffusion of once-nucleated particles across the particle boundary layer,.

1. INTRODUCTION

THE PROBLEM of mass transfer of a condensable vapor present in trace amounts in a relatively inert gaseous stream is encountered in many industrial processes. A few examples of recent interest are condensation of ash and K_2SO_4 seed in magnetohdrodynamic plants [1–4], deposition of ash and alkali sulfates on turbine blades in pressurized fluidized bed and direct coal-fired gas turbine applications [5, 6], and behavior of volatile fission products in light water reactors undergoing hypothetical core disruptive accidents [7, 8]. If the free stream is superheated, no mass transfer occurs until the surface attains the dew-point temperature. As the surface temperature is lowered further, the driving potential, i.e. the difference in partial pressure of the vapor and the saturation pressure at the wall temperature, increases, resulting in the enhanced rate of vapor mass transfer. On lowering the surface temperature still further, the saturation pressure being an exponential function of T_w (Clapeyron equation) approaches zero and the driving potential becomes independent of the wall temperature. For a constant property flow then, the mass transfer rate reaches a plateau becoming independent of the wall temperature.

The purpose of this paper is to extend the above understanding of mass transfer by including the role of boundary-layer nucleation. Below a certain wall temperature, one expects a portion of the boundary-layer next to the wall to become saturated giving rise to the possibility of vapor nucleation. In practice, a finite supersaturation is required to initiate the homogeneous nucleation process. Obviously, the onset of nucleation is accompanied by diminished vapor mass transfer rate. However, a compensating mechanism in the form of transport of the nucleated particles also comes into play. The particles are transported by Brownian diffusion and the thermophoretic force. The latter is important because of the temperature gradient at the wall and because the nucleated particles (being typically smaller than 20 Å) are amenable to thermophoretic transport. In turbulent boundary layers, the particles are also effectively transported by turbulent fluctuations. The question to be resolved here is: "How does boundary-layer nucleation and the subsequent transport of nucleated particles influence the mass transfer characteristics of a vapor present in trace amounts?"

Certain simplifications and approximations have been invoked while formulating the problem—e.g. the convection terms have been dropped from the conservation equations. The justification is that this represents a first attempt toward answering the question posed above and that the question is important and interesting in its own right. The approximations introduced should not bear any qualitative effect on the conclusions drawn here but only limit the applicability of the results. We intend to relax the approximations in future publications and to seek experimental verification of the results.

2. THEORY

We consider the convective flow of a stream, containing a trace amount of condensable impurity vapor, over a subcooled surface. The free stream is superheated with respect to the vapor whose concentration is sufficiently small to render negligible its effects on heat transfer and fluid mechanics. The unperturbed flow and temperature fields are assumed to be known from classical fluid mechanics. With reference to Fig. 1, a particle boundary-layer thickness δ_p is identified as the location where the gas temperature equals the dew-point temperature of the impurity vapor. Since the free stream is superheated, the particle boundary layer is within the flow boundary layer. For $y < \delta_p$, the gas is supersaturated so that the

NOMENCLATURE

D	diffusivity
J	homogeneous nucleation rate
k	Boltzmann constant
k_g	gas conductivity
Kn	Knudsen number
L_1	apparent latent heat
L_2	correction to Clapeyron equation
MW	molecular weight
n	distribution function
P	pressure
P_v	partial pressure of vapor
P_s	saturation pressure
Pr	Prandtl number
r	particle radius
r^*	critical radius
R	gas constant
S	supersaturation ratio
T	gas temperature
v	transverse velocity
$\hat{v}$	volume of a condensable molecule
W	flux
y	transverse direction
Y	mass fraction.

Greek symbols

δ	boundary-layer thickness
δ^*	incompressible displacement thickness
σ	surface tension
λ	mean free path
ν	kinematic viscosity
ρ	density
ρ_s	aerosol density
τ	shear stress.

Subscripts

B	Brownian
dp	dew point
l	liquid
p	particle
t	turbulent
th	thermophoretic
v	vapor
w	wall
∞	free stream.

vapor may nucleate and any nucleated particle will be stable. For $y > \delta_p$, the gas is superheated so that any particle diffused across the particle boundary layer will tend to vaporize. The following main assumptions have been made during the course of the analysis.

1. Explicit convection terms have been dropped from the conservation equations. The convection effects enter the problem implicitly through the boundary-layer parameters such as δ and temperature profile. This practice is routinely followed in estimating skin friction and heat transfer in turbulent flows [9].

2. The growth of the nucleated particles due to direct vapor condensation has been neglected. This is appropriate because we are dealing with a trace concentration of vapor and the particle growth rate is directly proportional to the partial vapor pressure.

3. The particles diffusing across the particle boundary layer are assumed to vaporize instantly. This is reasonable because the nucleated particles are expected to be smaller than 10 Å in radius so that the characteristic vaporization time should be extremely small. In general, the leaner the vapor concentration,

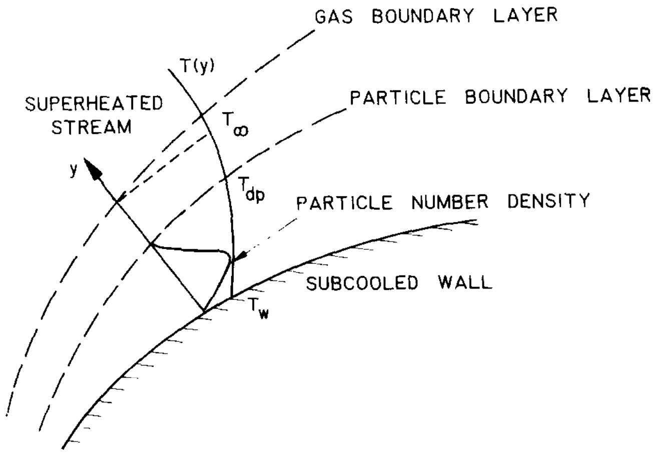

FIG. 1. Particle boundary layer for flow of a stream, superheated with respect to condensable trace vapor, over a subcooled surface.

the higher the supersaturation ratio required to initiate homogeneous nucleation, and the smaller is the critical size of the embryo and hence of the nucleated particles.

2.1. *Particle field*

The particles are nucleated from the impurity vapor in the region $y < \delta_p$. Neglecting convection (assumption 1), the particles are transported because of diffusion and thermophoresis. The resulting particle size distribution function is governed by the following conservation equation [1, 2, 10].

$$\frac{\partial}{\partial y}(v_{th} n) = \frac{\partial}{\partial y}\left(D_p \frac{\partial n}{\partial y}\right) + J\delta(r - r^*). \tag{1}$$

The particle size distribution function $n(r, y)\,dr$ is defined as the number of particles per unit volume in the size range r and $r + dr$. The boundary conditions for n are derived by requiring that n vanish at the surface because of strong Van der Waal's forces and at δ_p because of assumption 3.

$$n(r, 0) = 0 \tag{2}$$

$$n(r, \delta_p) = 0. \tag{3}$$

Homogeneous nucleation. According to the classical nucleation theory, the homogeneous nucleation rate is given by the following equation [1, 11].

$$J = \beta(4\pi r^{*2})ZN \exp(-\Delta G/kT) \tag{4}$$

where β is the collision rate of monomers of the impurity vapor with a flat surface, r^* the critical size of the embryo, Z the Zeldovich factor, N the concentration of the monomers and ΔG the change in Gibbs free energy due to the formation of the embryos. The critical size is given by the Gibbs–Thomson relationship:

$$r^* = \frac{2\sigma\hat{v}}{kT \ln S} \tag{5}$$

where S is the supersaturation ratio defined as

$$S = P_v/P_s. \tag{6}$$

Particle diffusion. In a laminar stream, the particle diffusivity is identical with the Brownian diffusivity (D_B) given by the Stokes–Einstein equation [11].

$$D_B = \frac{kTCn}{6\pi r\mu} \tag{7}$$

where Cn, the Cunningham correction factor, accounts for the slip between the particles and gas molecules when the particle size becomes of the same order as the mean free path.

$$Cn = 1 + Kn[1.257 + 0.4\exp(-1.1/Kn)] \tag{8}$$

$$Kn = \lambda/r. \tag{9}$$

In a turbulent stream, the effective diffusivity of the particles equals the sum of the Brownian and turbulent diffusivities. For the particle size of interest (less than 10 Å radius), the response frequency of the particles is higher than the frequency of the energy containing eddies. Thus, the particles can exactly follow the turbulent fluctuations, implying that the turbulent diffusivity of particles should equal the eddy diffusivity. Therefore,

$$D_p(r, y) = D_B(r, y) + v_t(y). \tag{10}$$

Thermophoresis. A particle suspended in a gas with an imposed temperature gradient experiences a thermal force producing motion directed toward lower temperatures. In the free molecular regime ($Kn \to \infty$) the thermophoretic velocity may be expressed as [11]

$$v_{th} = -0.1436\left(\frac{k_g}{P}\right)\frac{\partial T}{\partial y}. \tag{11}$$

The thermophoretic force is understood to result from the gas molecules in a temperature gradient field imparting more momentum to a suspended particle in a direction opposite to the temperature gradient than in direction of the gradient. This mechanism will be inoperative in the turbulent stream because of the random motion of the particle in an entrained eddy. Thus the thermophoretic velocity is considered nonzero in the laminar boundary layer and in the viscous sublayer of the turbulent boundary layer.

2.2. *Vapor field*

Neglecting the convection terms, the vapor mass fraction is given by the following conservation equations.

$$\frac{\partial}{\partial y}\left(\rho D_v \frac{\partial Y}{\partial y}\right) = 0, \qquad \delta_p < y < \delta \tag{12}$$

$$\frac{\partial}{\partial y}\left(\rho D_v \frac{\partial Y}{\partial y}\right) = \frac{4}{3}\pi\rho_l r^{*3} J, \qquad y < \delta_p. \tag{13}$$

The boundary conditions for equations (12) and (13) are:

$$Y(\delta) = Y_\infty \tag{14}$$

$$Y(\delta_p) = Y_s \tag{15}$$

$$Y(0) = Y_w \tag{16}$$

where Y_s, the vapor mass fraction at the edge of the particle boundary layer, is an unknown and will be determined from matching solutions. To a first approximation, the mass fraction Y_w may be simply related to the saturation pressure at the wall temperature.

$$Y_w = \frac{P_s(T_w)}{P}\left(\frac{MW_v}{MW}\right) \tag{17}$$

2.3. *Interface conditions*

The conservation of mass requires that the vapor flux at the edge of the particle boundary layer should be continuous. Recognizing assumption 3 stating that the particles crossing δ_p vaporize instantaneously, we have

$$\left(\rho D_v \frac{\partial Y}{\partial y}\right)^+ = \left(\rho D_v \frac{\partial Y}{\partial y}\right)^- + W_p(\delta_p) \tag{18}$$

where the superscript + refers to vapor diffusion from core toward δ_p and the superscript − to diffusion from δ_p toward the wall. The former quantity is calculated from equation (12) and the latter from equation (13). The particle flux is calculated by integrating the product of number flux and particle mass over the particle spectrum.

$$W_p(\delta_p) = \int_0^\infty \left(D_p \frac{\partial n}{\partial y} - v_{th} n \right) \frac{4}{3} \pi r^3 \rho_l \, dr. \qquad (19)$$

2.4. *Temperature field*

For a laminar boundary layer, given T_w, T_∞ and δ, we assume that the temperature profile is cubic.

$$\frac{T - T_w}{T_\infty - T_w} = \frac{3}{2}\left(\frac{y}{\delta}\right) - \frac{1}{2}\left(\frac{y}{\delta}\right)^3. \qquad (20)$$

For a turbulent flow, the boundary-layer profile is not symmetric with respect to y/δ only. Neglecting convection and assuming that the shear stress is constant within the boundary layer,

$$\tau_w = \rho(\nu + \nu_t) \frac{\partial u}{\partial y} \qquad (21)$$

from which it follows that

$$u = u_*^2 \int_0^y \frac{dy}{\nu + \nu_t} \qquad (22)$$

where u_* is the friction velocity

$$u_* = (\tau_w/\rho)^{1/2}. \qquad (23)$$

The turbulent eddy viscosity is calculated from the Van Driest model [12]. Accordingly, in the inner turbulent region

$$\frac{\nu_t}{\nu} = \frac{1}{2}\{[1 + 4l^{+2}]^{1/2} - 1\} \qquad (24)$$

where

$$l^+ = 0.4y^+[1 - \exp(-y^+/26)] \qquad (25)$$

and

$$y^+ = u_* y/\nu. \qquad (26)$$

In the outer turbulent region

$$\nu_t = 0.0168\, u_\infty \delta^*. \qquad (27)$$

For given u_∞, the shear velocity u_* is determined from equation (22) such that

$$u(\delta) = u_\infty. \qquad (28)$$

Knowing u_*, the turbulent eddy viscosity may be calculated from equations (23) and (26). Then, the temperature field may be calculated from the following equation.

$$\frac{T - T_w}{T_\infty - T_w} = \frac{\int_0^y dy/(\nu/Pr + \nu_t/Pr_t)}{\int_0^\delta dy/(\nu/Pr + \nu_t/Pr_t)}. \qquad (29)$$

The Stanton number is given as

$$St = \left[u_\infty \int_0^\delta dy/(\nu/Pr + \nu_t/Pr_t) \right]^{-1}. \qquad (30)$$

3. SOLUTION

3.1. *Particle field*

Equation (1) may be integrated once to relate the particle flux to the wall value.

$$D_p \frac{\partial n}{\partial y} - v_{th} n = \left(D_p \frac{\partial n}{\partial y} \right)_w - \int_0^y J \delta(r - r^*) \, d\xi. \qquad (31)$$

Integrating equation (31) a second time,

$$n(r, y) = \frac{N_p(0) \int_0^y \frac{I(\xi)}{D_p} d\xi - \int_0^y \frac{I(\xi)}{D_p} \left[\int_0^\xi J\delta(r - r^*) \, d\eta \right] d\xi}{I(y)} \qquad (32)$$

where

$$N_p(0) = \left(D_p \frac{\partial n}{\partial y} \right)_w \qquad (33)$$

and

$$I(y) = \exp\left[-\int_0^y \frac{v_{th}}{D_p} d\eta \right]. \qquad (34)$$

The wall flux $N_p(0)$ may be calculated by applying the boundary condition of equation (3) to equation (32).

$$N_p(0) = \frac{\int_0^{\delta_p} \frac{I(\xi)}{D_p} \left[\int_0^\xi J\delta(r - r^*) \, d\eta \right] d\xi}{\int_0^{\delta_p} \frac{I(\xi)}{D_p} d\xi}. \qquad (35)$$

In order to calculate the total particulate deposition flux, one has to integrate the product of N_p and particle mass over the particle size spectrum.

$$W_p(0) = \int_0^\infty \frac{4}{3} \pi r^3 \rho_l N_p(0) \, dr. \qquad (36)$$

A concise expression for $W_p(0)$ can be constructed by defining an average diffusivity ($\bar{D}_p$).

$$W_p(0) = \frac{\int_0^{\delta_p} \frac{\bar{I}(\xi)}{\bar{D}_p} \left[\int_0^\xi \frac{4}{3} \pi r^{*3} \rho_l J \, d\eta \right] d\xi}{\int_0^{\delta_p} \frac{\bar{I}(\xi)}{\bar{D}_p} d\xi} \qquad (37)$$

where

$$\bar{I}(y) = \exp\left[-\int_0^y \frac{\bar{v}_{th}}{\bar{D}_p} d\eta \right]. \qquad (38)$$

One can define an aerosol density ρ_s as

$$\rho_s(y) = \int_0^\infty \frac{4}{3} \pi r^3 \rho_l n(r, y) \, dr. \qquad (39)$$

Again, a concise expression for the aerosol density can be obtained by substituting equation (32) into (39) and using $\bar{D}_p$

$$\rho_s(y) = \frac{W_p(0)\int_0^y \frac{\bar{I}(\xi)}{\bar{D}_p}\,d\xi - \int_0^y \frac{\bar{I}(\xi)}{\bar{D}_p}\left[\int_0^\xi \frac{4}{3}\pi r^{*3}\rho_l J\,d\eta\right]d\xi}{\bar{I}(y)}. \tag{40}$$

Equation (31) can be used to determine the particle flux at any position:

$$N_p(y) = N_p(0) - \int_0^y J\delta(r-r^*)\,d\xi \tag{41}$$

from which the expression for particle mass flux at any position follows immediately.

$$W_p(y) = W_p(0) - \int_0^y \frac{4}{3}\pi r^{*3}\rho_l J\,d\xi. \tag{42}$$

Thus, the total vaporization rate of once-condensed particles is simply $W_p(\delta_p)$

$$W_p(\delta_p) = W_p(0) - \int_0^{\delta_p} \frac{4}{3}\pi r^{*3}\rho_l J\,d\xi. \tag{43}$$

3.2. *Vapor field*

The vapor mass fraction in the superheated region of the boundary layer, δ_p to δ, can be determined by twice integrating equation (12) and imposing the boundary condition of equations (14) and (15).

$$\frac{Y_\infty - Y}{Y_\infty - Y_s} = \frac{\int_y^\delta d\xi/\rho D_v}{\int_{\delta_p}^\delta d\xi/\rho D_v}. \tag{44}$$

The vapor flux in the superheated region is a constant.

$$W_v = (Y_\infty - Y_s)\Big/\int_{\delta_p}^\delta d\xi/\rho D_v. \tag{45}$$

In order to determine the vapor mass fraction in the supersaturated region of the boundary layer, 0 to δ_p, we twice integrate equation (13)

$$Y = Y_w + W_v(0)\int_0^y \frac{d\xi}{\rho D_v} + \int_0^y \frac{d\xi}{\rho D_v}\int_0^\xi \frac{4}{3}\pi r^{*3}\rho_l J\,d\eta. \tag{46}$$

The vapor flux at any position can be simply related to the wall value.

$$W_v(y) = W_v(0) + \int_0^y \frac{4}{3}\pi r^{*3}\rho_l J\,d\xi. \tag{47}$$

3.3. *Matching at interface*

The flux continuity condition, equation (18), may be used to calculate the vapor mass fraction at the interface. The various terms in this equation have already been determined and are reproduced below.

$$\left(\rho D_v \frac{\partial Y}{\partial y}\right)^+ = (Y_\infty - Y_s)\Big/\int_{\delta_p}^\delta d\xi/\rho D_v \tag{45'}$$

$$\left(\rho D_v \frac{\partial Y}{\partial y}\right)^- = W_v(0) + \int_0^{\delta_p} \frac{4}{3} r^{*3}\rho_l J\,d\xi \tag{47'}$$

$$W_p(\delta_p) = W_p(0) - \int_0^{\delta_p} \frac{4}{3}\pi r^{*3}\rho_l J\,d\xi. \tag{43}$$

Substituting the foregoing equations into equation (18), we have

$$Y_s = Y_\infty - [W_p(0) + W_v(0)]\int_{\delta_p}^\delta dy/\rho D_v. \tag{48}$$

3.4. *Numerics*

Equations (40), (45) and (46) describe the particle and vapor fields. The two fields are coupled because of the nucleation rate term appearing in the particle equation (35) and the $W_p(0)$ term appearing in the vapor equation (48). The solution requires iteration because $W_v(0)$, the vapor deposition flux at wall, appears in equation (46) and this quantity is not known *a priori*. The following iteration scheme has been found to be convenient and convergent.

(a) Guess $W_v(0)$.
(b) Calculate the vapor mass fraction (Y) in the region 0 to δ_p from equation (46). Note that

$$Y_s = Y(\delta_p). \tag{15}$$

(c) Calculate the vapor flux at δ_p from equation (47).
(d) Calculate the vapor mass fraction in the region δ_p to δ from equation (44) and the vapor flux at δ_p from equation (45).
(e) Calculate $W_p(0)$ from equation (37) and the aerosol density from equation (40).
(f) Calculate $W_p(\delta_p)$ from equation (43).
(g) Check if equation (13) is satisfied. If not, use this equation to update a guess for $W_v(0)$. The update may be obtained by the Newton–Raphson method. Repeat steps (a)–(f) until equation (13) is satisfied to the desired tolerance.

4. RESULTS AND DISCUSSION

Illustrative calculations have been performed for deposition of trace Na_2SO_4 vapor on a subcooled surface. Air is assumed to be the gaseous medium whose density is approximated by the equation of state for ideal gases, viscosity by Sutherland's equation, and thermal conductivity as directly proportional to the gas temperature. The product of gas density and molecular diffusivity is taken as constant (6.75×10^{-5} kg m^{-1} s^{-1}), and the liquid density as 2680 kg m^{-3}. The free-stream velocity and temperature are 5 m s^{-1} and 1350 K, respectively, and the pressure is atmospheric. The nominal boundary-layer thickness is 5 cm for laminar flow calculations and 10 cm for the turbulent flow.

4.1. *Laminar flow*

Figure 2 illustrates the influence of surface subcooling on the deposition flux. The broken line represents the pure vapor deposition flux (W_{vp}) obtained when the boundary-layer nucleation is ignored and is given by the following equation.

$$W_{vp} = (Y_\infty - Y_w) \Big/ \int_0^\delta d\xi/\rho D_v. \tag{49}$$

As the surface is sufficiently subcooled, Y_w becomes small and W_{vp} approaches the asymptotic value of $Y_\infty / \int_0^\delta d\xi/\rho D_v$. Since the product ρD_v is a constant, the limiting value of W_{vp} is also a constant, $\rho D_v Y_\infty/\delta$. The deposition behavior changes markedly upon inclusion of boundary-layer nucleation. There is a critical surface temperature at which departure occurs and the nucleation effect is felt. Below the critical temperature, the homogeneous nucleation of vapor is initiated which depresses the local mass fraction of the vapor and hence the vapor deposition flux. At the same time, the deposition of nucleated particles comes into play, more than compensating for the decrease in vapor deposition flux. The net particle plus vapor deposition flux exceeds the asymptotic value of the pure vapor deposition flux.

Figure 3 shows the depression in vapor mass fraction due to homogeneous nucleation. The nondimensional mass fraction profile across the boundary layer approaches a straight line as the surface temperature nears the dew point. The maximum deviation from the straight-line profile occurs within the particle boundary layer. The difference in mass fraction, when nucleation is considered from the case when it is neglected, can be written as follows (for constant ρD_v).

$$\Delta Y = Y(\text{no nucleation}) - Y(\text{with nucleation})$$

$$= \frac{y}{\rho D_v}(W_{vp} - W_v) - \frac{1}{\rho D_v}\int_0^y d\xi \left[\int_0^\eta \frac{4}{3}\pi r^{*3} \rho_l J \, d\eta\right]. \tag{50}$$

The location of maximum ΔY is obtained by setting its first derivative with respect to y equal to zero and noting that the second derivative is always negative. Then, it follows that the location of maxima is such that the integrated nucleation rate equals the difference between the vapor deposition fluxes for the cases of without and with nucleation.

$$\int_0^{y_{\max}} \frac{4}{3}\pi r^{*3} \rho_l J \, d\xi = W_{vp} - W_v. \tag{51}$$

By back substitution it also follows that

$$\Delta Y_{\max} = \frac{1}{\rho D_v}\int_0^{y_{\max}} \frac{4}{3}\pi r^{*3} \rho_l J \xi \, d\xi. \tag{52}$$

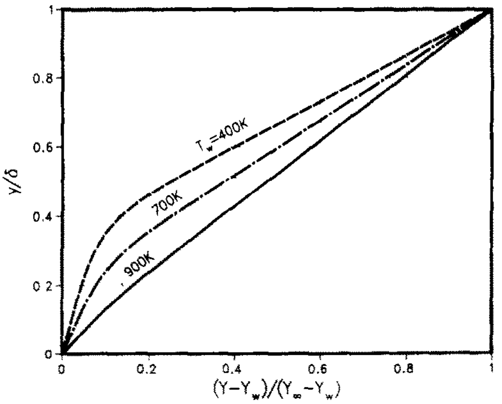

Fig. 3. Effect of boundary-layer nucleation on the mass fraction profile of condensable vapor in laminar flow.

Figure 4 shows the variation of aerosol density across the particle boundary layer whose thickness is a function of surface temperature: $\delta_p/\delta = 0.80$ for $T_w = 400$ K, 0.76 for $T_w = 700$ K and 0.70 for $T_w = 900$ K. The aerosol density becomes vanishingly small well within δ_p. This is because the laminar temperature profile changes slowly, and since a large supersaturation is required to initiate homogeneous nucleation of trace species the critical temperature lies deep within δ_p. Thus, there is an insignificant diffusion of once-

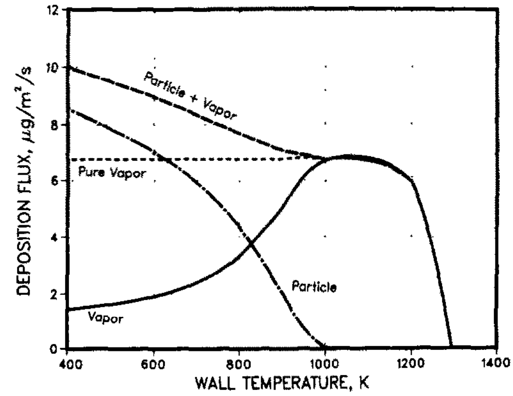

Fig. 2. Variation of particle and vapor deposition flux with surface subcooling in laminar flow.

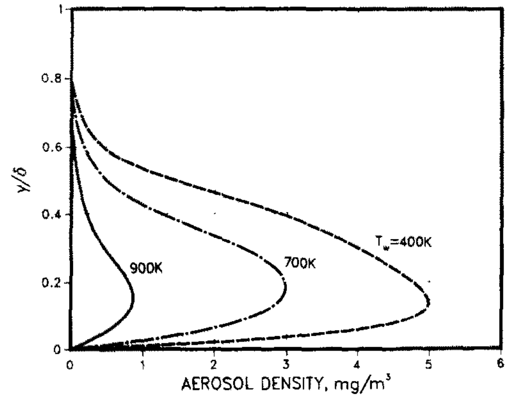

Fig. 4. Spray density profile across the laminar boundary layer.

condensed particles out of δ_p, i.e. $W_p(\delta_p) = 0$. Therefore, the nucleation rate integrated over δ_p equals the particle deposition flux, equation (43).

$$W_p(0) = \int_0^{\delta_p} \frac{4}{3}\pi r^{*3}\rho_l J \, d\xi. \qquad (53)$$

It is observed in Fig. (4) that the maxima of ρ_s lies close to the wall. The location and magnitude of the maxima can be obtained by combining equations (40) and (53).

$$\rho_s(y_{max}) = -\frac{1}{v_{th}(y_{max})}\int_{y_{max}}^{\delta} \frac{4}{3}\pi r^{*3}\rho_l J \, d\eta \qquad (54)$$

4.2. *Turbulent flow*

For turbulent flow, all properties $(\rho, D_v, D_B, k_g, \mu)$ have been calculated at the reference temperature defined as [13]

$$T_{ref} = 0.28\ T_\infty + 0.72\ T_w. \qquad (55)$$

Figure 5 shows the effect of surface subcooling on the deposition flux from a turbulent stream. As for a laminar stream, there is a critical surface temperature below which the vapor deposition flux begins to decrease with surface subcooling. There is another critical temperature below which the particle deposition flux exceeds its vapor counterpart. Unlike the laminar flow case, the pure vapor deposition flux does not become a constant at very low wall temperatures. This is because of the temperature dependence of the physical properties. Note that the Reynolds number based on properties at reference temperature increases with subcooling and so does the vapor deposition flux. Another distinct feature of turbulent flow is that the total deposition flux, particle plus vapor, is lower than that calculated when the boundary-layer nucleation is ignored. This is because a significant fraction of the once-condensed particles diffuse across the particle boundary layer and are revaporized, Fig. 6.

Figure 5 also points to the existence of a 'knee' in the deposition curve. The deposition flux initially increases with surface subcooling because of the enhancement in vapor deposition rate. It decreases subsequently because of boundary-layer nucleation suppressing the vapor deposition flux. On further lowering of wall temperature, it increases again because of the augmented thermophoretic deposition of nucleated particles.

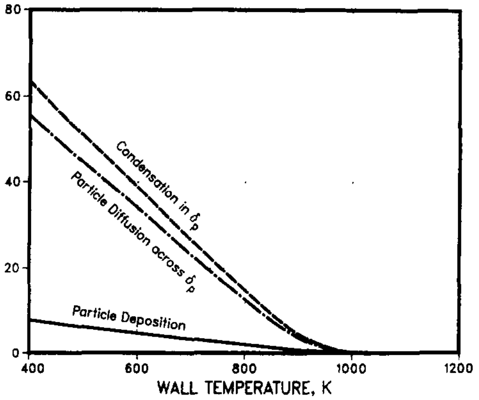

FIG. 6. Effect of surface subcooling on the relative amounts of nucleated particles diffusing across δ_p and depositing on the wall. The flow field is turbulent.

Figures 7 and 8 show the boundary-layer profiles of nondimensional vapor mass fraction and the aerosol density. Except for the turbulent nature of the profiles, the results in Fig. 7 are qualitatively similar to those in Fig. 3 for laminar flow. The aerosol density profile in Fig. 8 is characteristically different from its laminar counterpart in that a non-zero value of ρ_s persists up to the edge of the particle boundary layer. This results in a significant diffusion of once-condensed particles out of δ_p, Fig. 6, and in $W_p(0)$ being much smaller than the condensation rate in the boundary layer.

4.3. *Criterion for appearance of fog*

With reference to Figs. 2 and 5, a critical wall temperature can be identified below which vapor

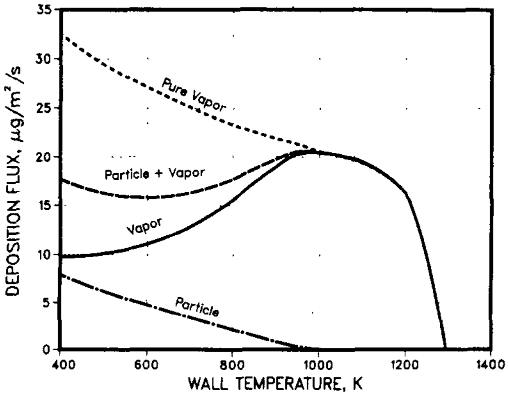

FIG. 5. Variation of particle and vapor deposition flux with surface subcooling in turbulent flow.

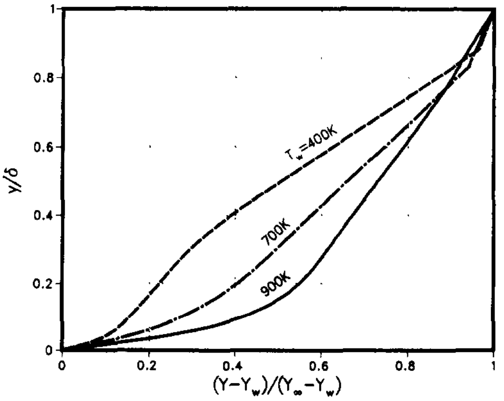

FIG. 7. Effect of boundary-layer nucleation on the turbulent mass fraction profile of condensable vapor.

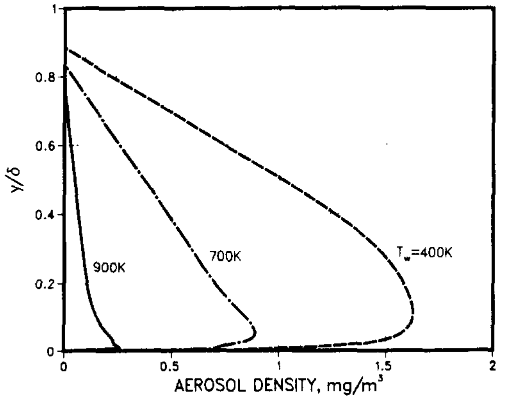

FIG. 8. Spray density profile across the turbulent boundary layer.

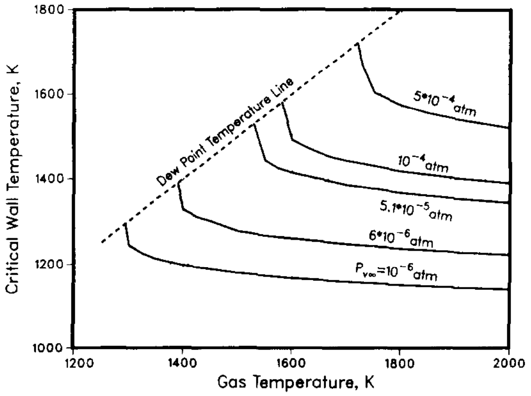

FIG. 9. Critical wall temperature that renders the boundary layer just supersaturated.

deposition flux begins to decrease with subcooling. In as much as the decrease is associated with the boundary-layer nucleation, this critical condition may also serve as the criterion for the appearance of fog. Mathematically, the critical wall temperature is such that

$$\frac{\partial W_v(0)}{\partial T_w} = 0 \tag{56}$$

and

$$\frac{\partial^2 W_v(0)}{\partial T_w^2} > 0. \tag{57}$$

The foregoing criterion is a kinetic one since the kinetics of the nucleation process is already factored in its definition. It is also possible to derive a thermodynamic criterion for fog formation. Following the arguments put forth by Johnstone *et al.* [14], the thermodynamic requirement is that at critical temperature, the slopes of the gas and dew-point temperature profiles be equal.

$$\left(\frac{\mathrm{d}T}{\mathrm{d}y}\right)_w = \left(\frac{\mathrm{d}T_{dp}}{\mathrm{d}y}\right)_w \tag{58}$$

where

$$\left(\frac{\mathrm{d}T_{dp}}{\mathrm{d}y}\right)_w = \left(\frac{\mathrm{d}P_v}{\mathrm{d}y}\right)_w \Big/ \left(\frac{\mathrm{d}P_v}{\mathrm{d}T_{dp}}\right)_w. \tag{59}$$

It is instructive to confine the analysis to laminar flow for which the gas temperature and mass fraction profiles are given by equations (20 and (46), respectively. For constant ρD_v and the following saturation pressure–temperature relationship,

$$\frac{\mathrm{d}P_s}{\mathrm{d}T} = P_s\left(\frac{L_1}{RT^2} + \frac{2L_2}{RT^3}\right) \tag{60}$$

it follows that the critical wall temperature is implicity given by the following equation.

$$\left(\frac{P_{v\infty}}{P_{sw}} - 1\right) = \frac{3}{2}\left(\frac{T_\infty}{T_w} - 1\right)\left(\frac{L_1}{RT_w} + \frac{2L_2}{RT_w^2}\right) \tag{61}$$

where P_{sw} is the saturation pressure at the wall temperature. The critical temperature has been plotted in Fig. 9 as a function of the gas temperature and the free-stream partial pressure.

The thermodynamic criterion essentially determines the wall temperature such that the gas becomes just supersaturated. The correct interpretation of the wall temperature so determined is that no fog can form above this temperature. A finite supersaturation is required to initiate boundary-layer nucleation. Therefore, the kinetic criterion, equation (56), provides the correct temperature for appearance of fog. Naturally, the kinetic criterion stipulates that the wall be undercooled below the thermodynamically determined value before fog can be formed. Moreover, the critical temperature is a function of not only the gas temperature and the free-stream partial pressure but also of flow Reynolds number and surface tension, etc. For the conditions of Fig. 2 ($T_\infty = 1350$ K, $P_{v\infty} \simeq 10^{-6}$ atm), the critical wall temperature is 1000 K—nearly 210 K below the 1210 K temperature calculated from the thermodynamic criterion, Fig. 9.

5. CONCLUSIONS

The mass transfer of a trace species from a superheated stream to a subcooled surface is affected by boundary-layer nucleation. It acts as an inhibitor to mass transfer from a turbulent stream but as a promoter if the flow field is laminar. The effect of boundary-layer nucleation is to decrease the vapor mass fraction and hence the vapor deposition flux. For laminar flow, this is compensated by deposition of nucleated particles with the resultant total deposition flux, particle plus vapor, exceeding the pure vapor deposition flux. For turbulent flow, the decrease in vapor deposition flux due to boundary-layer nucleation is not compensated by the ensuing particle deposition partly because of turbulent diffusion of once-nucleated particles across the particle boundary layer. The emerging picture is that for laminar flow the mass transfer increases with surface subcooling, whereas for turbulent flow there is an intermediate range where it decreases with surface cooling.

There is a critical degree of subcooling required to initiate the boundary-layer nucleation. The required minimum can be determined from the equilibrium thermodynamics based on traditional concepts of heat and mass transfer. The actual required subcooling is higher because of the nucleation kinetics and can be estimated from the simplified model formulated in this work.

Further work is required to refine the boundary-layer nucleation model. In particular, the assumptions leading to the neglect of convection terms in the governing equations and the growth of nucleated particles need to be relaxed. The former limits the accuracy of the results whereas the latter restricts the applicability of the model to the condensation of trace species.

REFERENCES

1. K. H. Im and P. M. Chung, Nucleation and evolution of slag droplets in coal combustion, *A.I.Ch.E. Jl* **28,** 655–663 (1980).
2. K. H. Im and R. K. Ahluwalia, Nucleation of slag and seed in MHD plants, 20th Symposium on Engineering Aspects of Magnetohydrodynamics, Irvine, California (1982).
3. R. K. Ahluwalia and K. H. Im, Aerosol and vapor deposition of slag and seed in MHD components, 20th Symposium on Engineering Aspects of Magnetohydrodynamics, Irvine, California (1982).
4. J. B. Heywood and G. J. Womack, *Open-Cycle MHD Power Generation.* Pergamon Press, Oxford (1969).
5. R. K. Ahluwalia, K. H. Im, C. F. Chuang, H. K. Geyer, T. J. O'Brien, G. F. Berry, K. M. Myles and M. Petrick, Behavior of coal ash and alkali matter in a coal-fired gas turbine system, 84-GT-217, 29th International Gas Turbine Conference, Amsterdam, The Netherlands (1984).
6. D. E. Rosner, B. K. Chen, G. F. Fryburg and F. J. Kohl, Chemically frozen multicomponent boundary layer theory of salt and/or ash deposition rates from combustion gases, *Int. J. Heat Mass Transfer* **20,** 87–106 (1979).
7. K. H. Im, R. K. Ahluwalia and C. F. Chuang, RAFT: a computer model for formation and transport of fission product aerosols in LWR primary systems, ANS Topical Meeting on Fission Product Behavior and Source Term Research, Snowbird, Utah (1984).
8. Technical Bases for Estimating Fission Product Behavior During LWR Accidents, NUREG-0772, U.S. Nuclear Regulatory Commission (June 1981).
9. W. M. Kays, *Convective Heat and Mass Transfer.* McGraw-Hill, New York (1966).
10. K. H. Im and P. M. Chung, Particulate deposition from turbulent parallel streams, *A.I.Ch.E. Jl* **29,** 498–505 (1983).
11. G. M. Hidy and J. R. Brock, *The Dynamics of Aerocolloidal Systems.* Pergamon Press, Oxford (1970).
12. T. Cebeci and A. M. O. Smith, *Analysis of Turbulent Boundary Layers.* Academic Press, New York (1974).
13. W. M. Rosenhow and J. P. Hartnett, *Handbook of Heat Transfer.* McGraw-Hill, New York (1973).
14. H. F. Johnstone, M. D. Kelley and L. D. McKinley, Fog formation in cooler condenser, *Ind. Engng Chem.* **42,** 2298–2302 (1950).

TRANSFERT MASSIQUE D'ESPECES EN TRACE DEPUIS UN ECOULEMENT SURCHAUFFE VERS UNE SURFACE SOUS-REFROIDIE

Résumé—On analyse l'influence sur le transfert massique de la nucléation en couche limite despèces condensables allant d'une vapeur surchauffée à une surface sous-refroidie. L'espèce est suffisamment diluée pour éviter toute condensation sur les particules nucléées. On trouve qu'une forte sursaturation est nécessaire pour initier la nucléation en couche limite. Il en résulte que la température critique de surface pour le début de nucléation et l'apparition du brouillard est bien en dessous de celle déterminée à partir des critères thermodynamiques. Le transfert massique de la vapeur est toujours diminué par la nucléation en couche limite. Le dépôt de particules nucléées lors de l'écoulement laminaire est plus que compensé par rapport à cette diminution de telle façon que le transfert thermique—vapeur plus particules—dépasse la valeur obtenue en négligeant la nucléation. Pour l'écoulement tubulent, le transfert massique net décroît avec la nucléation en couche limite, en partie à cause de la diffusion turbulente des particules nucléées à travers la couche limite de particules.

STOFFÜBERTRAGUNG VON SPURENELEMENTEN VON EINEM ÜBERHITZTEN DAMPFSTROM AN EINE UNTERKÜHLTE OBERFLÄCHE

Zusammenfassung—Es wurde der Einfluß der Kristallisation in der Grenzschicht auf die Stoffübertragung von kondensierbaren Spurenelementen aus einem überhitzten Dampfstrom an eine unterkühlte Oberfläche untersucht. Die Konzentration der Spurenelemente ist ausreichend gering, um jegliche Kondensation an den kristallisierten Teilchen zu verhindern. Es wurde festgestellt, daß ein hohes Übersättigungs-Verhältnis erforderlich ist, um die Kristallisation in der Grenzschicht auszulösen. In Konsequenz daraus hat sich ergeben, daß die kritische Oberflächentemperatur für das Einsetzen der Kristallisation und das Auftreten von Nebel wesentlich niedriger ist also die nach einem thermodynamischen Kriterium bestimmte. Der Stofftransport des Dampfes wird durch die Kristallisation in der Grenzschicht verringert. Durch das anschließende Ablagern von kristallisierten Teilchen in einer laminaren Strömung wird die Abnahme mehr als kompensiert, so daß der Netto-Stofftransport—Dampf und Partikel—den Wert überschreitet, der bei Vernachlässigung der Kristallisation erreicht würde. Für turbulente Strömung nimmt der Netto-Stofftransport aufgrund der Kristallisation in der Grenzschicht ab. Dies rührt teilweise von der turbulenten Diffusion durch plötzlich kristallisierende Teilchen entlang der Partikelgranzschicht her.

МАССОПЕРЕНОС ИНДИКАТОРНЫХ ВЕЩЕСТВ ИЗ ПЕРЕГРЕТОГО ПОТОКА НА НЕДОГРЕТУЮ ПОВЕРХНОСТЬ

Аннотация—Анализируется влияние нуклеации в пограничном слое на массоперенос индикаторных конденсирующихся веществ из перегретого потока на недогретую поверхность. Для предотвращения конденсации молекул индикаторного вещества на появившихся зародышах новой фазы концентрация пара была очень низкой. Найдено, что для инициирования нуклеации в пограничном слое необходима большая степень пересыщения. Как следствие, критическая температура поверхности, необходимая для начала нуклеации и появления тумана, намного ниже определенной из термодинамического критерия. Перенос пара всегда уменьшается вследствие нуклеации в пограничном слое. Последующее оседание частиц, возникших в ламинарном потоке, значительно компенсирует уменьшение переноса в газовой фазе, так что суммарный массоперенос (пар плюс частица) превышает значение, полученное без учета нуклеации. В результате нуклеации в пограничном слое, для турбулентного потока суммарный массоперенос уменьшается частично из-за турбулентной диффузии уже образовавшихся частиц поперек пограничного слоя.